THE JOURNAL OF PHYSICAL CHEMISTRY A
A JOURNAL OF THE AMERICAN CHEMICAL SOCIETY

pubs.acs.org/JPCA

Article

Anion-Activated Bases and Nucleophiles Characterized by Photoelectron Spectroscopy

Stephen H. Dempsey, Wenjin Cao, Xue-Bin Wang,* and Steven R. Kass*

Cite This: J. Phys. Chem. A 2023, 127, 8828−8833

Read Online

ACCESS | Metrics & More | Article Recommendations | Supporting Information

ABSTRACT: Negative ion photoelectron spectra at 20 K along with ab initio [CCSD(T)] and M06-2X density functional theory calculations are reported for a series of six basic and nucleophilic pyridine derivatives with an anionic substituent [i.e., 3- and 4-PyrBX$_3^-$, where X = F, 4-*t*-BuC_6H_4, 4-MeOC_6H_4, and 3,5-$(MeO)_2C_6H_3$]. Vertical detachment energies (VDEs) of these charge-activated reagents span from 4.50−5.85 eV and are well reproduced by M06-2X/aug-*cc*-pVTZ and CCSD(T)/maug-*cc*-pVTZ computations. Surprisingly, the VDEs are found to correlate with the S_N2 reactivity of the PPh_4^+ salts of the substituted pyridine anions with 1-iodooctane in dichloromethane. This provides an experimental measure of the nucleophilicity of these charge-activated anions, which represent a new class of chemical reagent.

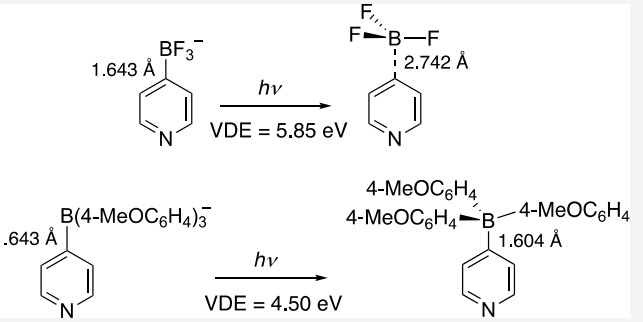

Downloaded via UNIV OF MINNESOTA on June 14, 2024 at 15:43:46 (UTC).
See https://pubs.acs.org/sharingguidelines for options on how to legitimately share published articles.

INTRODUCTION

Electric fields can impact bond energies and a wide range of chemical transformations.[1−5] One general application that has been explored over the past decade is the incorporation of a positively charged substituent into a neutral Brønsted acid so as to enhance its acidity and catalytic abilities.[6−23] Conversely, one would expect that a negatively charged substituent can be used to increase the basicity and nucleophilicity of a noncharged Brønsted base since a positive charge builds up at the basic or nucleophilic site. Given the tremendous importance of bases and nucleophiles in biological and industrial processes including the synthesis of pharmaceutical and agrochemicals,[24−31] we decided to investigate these species.

A series of tetraphenylphosphonium salts including 3- and 4-pyridyltrifluoroborates (**1** and **2**, respectively) and their triaryl analogues **3**−**6** (Scheme 1) were prepared and studied.[32] The S_N2 reaction of the tetraphenylphosphonium salt of 3-pyridyltri(4-*t*-butylphenyl)borate (**3**) with 1-iodooctane (eq 1) was found to proceed 10 times faster than the activated noncharged pyridine derivative known as DMAP (i.e., 4-dimethylaminopyridine). It also reacts 6 times faster than DMAP in their base-catalyzed urethane forming reaction with 1-butanol and 4-methylphenylisocyanate (eq 2).[32,33] These compounds represent a new class of reagents, and to increase the reactivity of such species, the interaction of the oppositely

Scheme 1. Charge-Activated Borate Salts Studied in This Work

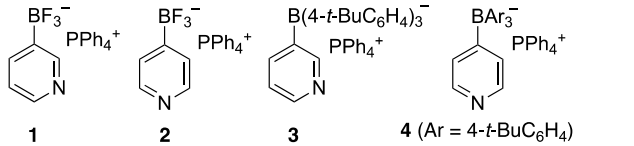

1 **2** **3**

4 (Ar = 4-*t*-BuC_6H_4)
5 (Ar = 4-MeOC_6H_4)
6 (Ar = 3,5-$(MeO)_2C_6H_3$)

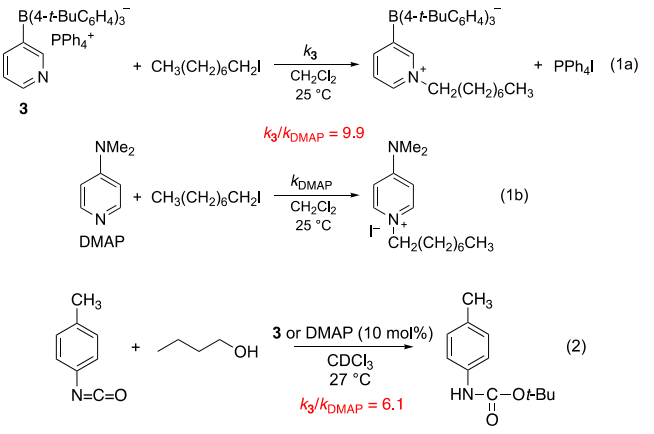

Received: July 3, 2023
Revised: September 25, 2023
Published: October 16, 2023

ACS Publications

© 2023 American Chemical Society

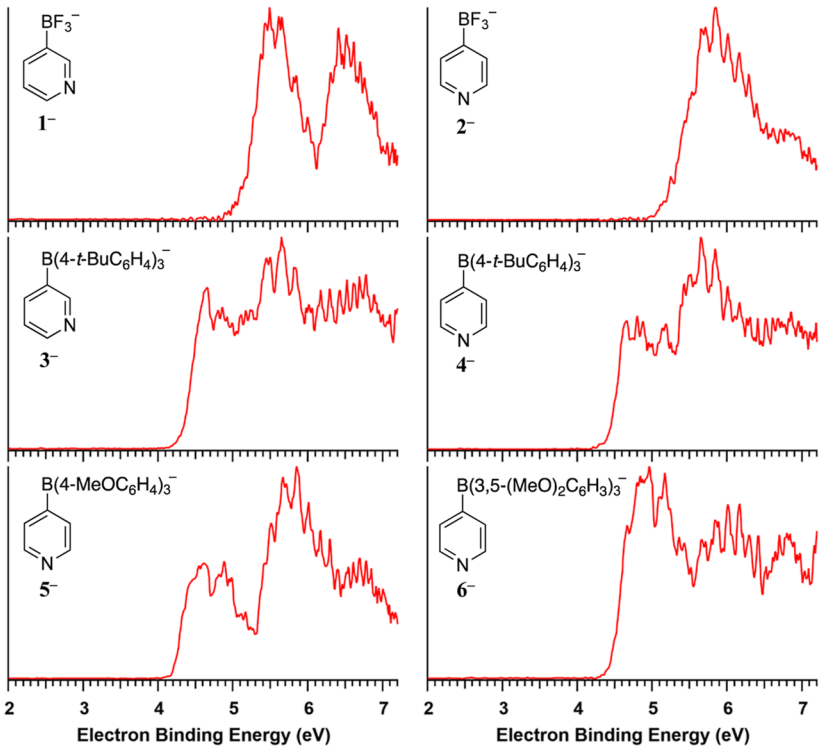

Figure 1. NIPE spectra of 1^-−6^- recorded at 157.6 nm and 20 K.

Table 1. Experimental and Calculated VDEs of Borate Anions 1^-−6^- and Their Computed Fragmentation Energies

	VDE (eV)[a]				ΔH_{Diss}° (0 K)[c]	ΔH_{Diss}° (0 K)[c]
cmpd	sp	opt	CCSD(T)	expt (eV)[b]	anion	radical
1	5.79	5.72	5.60	5.50 or 5.64	75.9 (75.8) [74.1]	4.6 (4.2) [2.7]
2	5.92	5.84	5.77	5.85	75.1 (75.1) [73.4]	4.5 (4.1) [2.5]
3	4.74	4.77		4.65	77.7 (75.3) [75.2][d]	15.4 (12.3) [12.2][d]
4	4.77	4.76		4.66	77.5 (75.0) [74.4][e]	14.1 (10.9) [10.8][e]
5	4.52	4.51		4.50		
6	4.85	4.84		4.90		

[a]sp = M06-2X/aug-*cc*-pVTZ//M06-2X/aug-*cc*-pVDZ, opt = M06-2X/aug-*cc*-pVTZ, and CCSD(T) = CCSD(T)/maug-*cc*-pVTZ//M06-2X/aug-*cc*-pVTZ. [b]Estimated uncertainties are ±0.10 eV. [c]ΔH_{Diss}° = M06-2X/aug-*cc*-pVTZ//M06-2X/aug-*cc*-pVDZ, (M06-2X/aug-*cc*-pVTZ), and [CCSD(T)/maug-*cc*-pVTZ] values in kcal mol^{-1}. [d]These values are for 3-PyrBPh$_3^-$ and its corresponding radical. [e]These values are for 4-PyrBPh$_3^-$ and its corresponding radical.

charged ions presumably needs to be weakened. Therefore, we decided to probe where the excess electron density resides in the free and unencumbered borate anions derived from salts **1**−**6** by carrying out DFT and CCSD(T) computations in conjunction with negative ion photoelectron spectroscopy (NIPES) studies.

METHODS

Experiments. NIPES was carried out using an instrument that previously has been described.[34] It consists of a magnetic bottle time-of-flight photoelectron spectrometer with an electrospray ionization source and a cryogenic ion trap. In this work, ∼ 0.1 mM solutions of **1**−**6** dissolved in 1:3 H_2O/CH_3CN or CH_3CN were used to generate the borate anions of interest. Accumulation of these ions for 20−100 ms in the cryogenic 3D ion trap enabled them to be cooled to 20 K by collisions with a helium buffer gas. The anions were subsequently pulsed into the time-of-flight mass spectrometer at a repetition rate of 10 Hz, where they were mass-selected and decelerated for photodetachment with a 157.6 nm (7.866 eV) Lambda Physik CompexPro 100 F2 laser operated at 20 Hz. In this way, photoelectron spectra were recorded with the ion beam on and off on alternating laser shots to obtain shot-to-shot background corrected spectra. The resulting photoelectrons were collected at nearly 100% efficiency and analyzed with a 5.2 m long flight tube. Their measured flight times were then converted into calibrated kinetic energies using the known spectrum of $I^-/Au(CN)_2^-$.[35,36] Vertical detachment energies (VDEs) were subsequently obtained from the peak maxima of the first observed band in the photoelectron spectrum and have an estimated energy resolution ($\Delta E/E$) of about 2% or ∼20 meV at 1 eV.

Computations. Geometry optimizations were carried out using the M06-2X[37−39] hybrid functional along with the aug-*cc*-pVDZ basis set starting with previously reported structures,[32] and subsequently were reoptimized with the larger aug-*cc*-pVTZ basis set.[40] Vibrational frequencies were computed for all of the aug-*cc*-pVDZ and some of the aug-*cc*-pVTZ structures to obtain zero-point energies and to confirm that they correspond to stationary points on the potential energy

https://doi.org/10.1021/acs.jpca.3c04479
J. Phys. Chem. A 2023, 127, 8828−8833

surface. Refined M06-2X/aug-*cc*-pVTZ//M06-2X/aug-*cc*-pVDZ and CCSD(T)/maug-*cc*-pVTZ//M06-2X/aug-*cc*-pVTZ[41−43] single-point energies were also computed and used to obtain VDEs, which correspond to the energy differences between the anions and their corresponding radicals with the geometry of the anion. To save computational resources, the truncated maug-*cc*-pVTZ basis set developed by Papajak and Truhlar was used instead of the larger aug-*cc*-pVTZ basis set for the CCSD(T) calculations.[41] Reference compounds including trifluoroborane, triphenylborane, 3- and 4-pyridyl anions, and their corresponding radicals were also computed to obtain 0 K enthalpies for the fragmentation of BF_3 from $\mathbf{1}^-$, $\mathbf{2}^-$, and their corresponding radicals. Cleavage of BPh_3 from 3- and 4-pyridyltriphenylborate anion and neutral was determined as well. The Gaussian 16[44] suite of programs was used to carry out all of these computations at the Minnesota Supercomputer Institute for Advanced Computational Research and Gaussview 6[45] was used to visualize radical spin densities and frontier molecular orbitals.

RESULTS AND DISCUSSION

Negative ion photoelectron spectra of the borate anions derived from **1**−**6** were obtained at 20 K (Figure 1). All six spectra are broad and show multiple features with VDEs ranging from 4.50 ± 0.1−5.85 ± 0.1 eV. The lower values are for the triarylborate derivatives, and the higher binding energies are for the trifluoroborates (Table 1). For 3-pyridyltrifluoroborate ($\mathbf{1}^-$, Figure 1), there are two features in the first (low energy) band at 5.50 and 5.64 eV with essentially the same intensities. In this case, either value could correspond to the VDE.

Structures for $\mathbf{1}^-$−$\mathbf{6}^-$ were previously examined and provided the starting geometries for the optimizations and single-point energy calculations carried out in this work.[32] Interestingly, M06-2X/aug-*cc*-pVTZ geometries of the neutral structures derived from $\mathbf{1}^-$ and $\mathbf{2}^-$ have elongated C−B distances of 2.739 and 2.742 Å compared to 1.635 and 1.636 Å bond lengths in their respective anions (Figure 2). The BF_3 substituent also flattens out in the radical and becomes almost planar with FBFF dihedral angles of 118.6 and 175.3° in $\mathbf{1}^-$ and $\mathbf{1}^\bullet$, respectively, and 119.4 and 175.4° for $\mathbf{2}^-$ and $\mathbf{2}^\bullet$. This suggests that the interaction of BF_3 with the aromatic rings is much stronger in the anions than in the corresponding radicals and that in the latter case the association is a weak one. Consistent with these inferences based upon the geometry changes, CCSD(T)/maug-*cc*-pVTZ//M06-2X/aug-*cc*-pVTZ [referred to as CCSD(T) hereafter] 0 K dissociation enthalpies of 74.1 ($\mathbf{1}^-$) and 73.4 ($\mathbf{2}^-$) kcal mol^{-1} were obtained as opposed to 2.7 and 2.5 kcal mol^{-1} for the respective radicals.

CCSD(T) VDEs for $\mathbf{1}^-$ and $\mathbf{2}^-$ are 5.60 and 5.77 eV, respectively. These values and the respective M06-2X/aug-*cc*-pVTZ VDEs of 5.72 and 5.84 eV are in excellent agreement with the corresponding experimental assignments of 5.64 and 5.85 eV; in the former case, there is also a band at 5.50 eV with essentially the same intensity that could be assigned as the VDE, but the larger value is in better accord with both the CCSD(T) and M06-2X results. Adiabatic detachment energies (ADEs) correspond to the energy difference between the ground state of an anion and the ground state of its corresponding radical, and when there is a large geometry difference between the two, an extended progression with weak Franck−Condon factors may be observed. This leads to onset energies that correspond only to upper bounds for the ADEs.

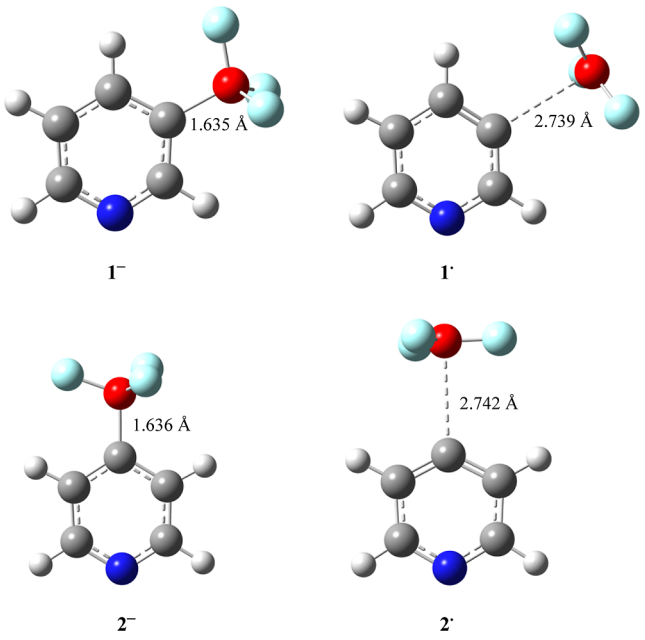

Figure 2. Optimized M06-2X/aug-*cc*-pVTZ structures of 3-PyrBF_3^- ($\mathbf{1}^-$), 3-Pyr$BF_3^\bullet$ ($\mathbf{1}^\bullet$), 4-PyrBF_3^- ($\mathbf{2}^-$), and 4-Pyr$BF_3^\bullet$ ($\mathbf{2}^\bullet$) with distances in Å.

Our assigned values of ≤4.9 eV for both $\mathbf{1}^-$ and $\mathbf{2}^-$ are ∼0.4 eV greater than the calculated CCSD(T) ADEs of 4.48 ($\mathbf{1}^-$) and 4.49 ($\mathbf{2}^-$) eV which is in keeping with the large computed geometry changes occurring upon electron loss from both anions.

3- and 4-Pyridyltriarylborate anions $\mathbf{3}^-$−$\mathbf{6}^-$ have similar M06-2X/aug-*cc*-pVTZ geometries to the trifluoroborate derivatives (Figure S1), but the corresponding radicals which were initially modeled without the phenyl ring substituents (i.e., 3-Pyr$BPh_3^\bullet$ and 4-Pyr$BPh_3^\bullet$) are quite different (Figure 3). That is, the BPh_3 group does not elongate or flatten out but

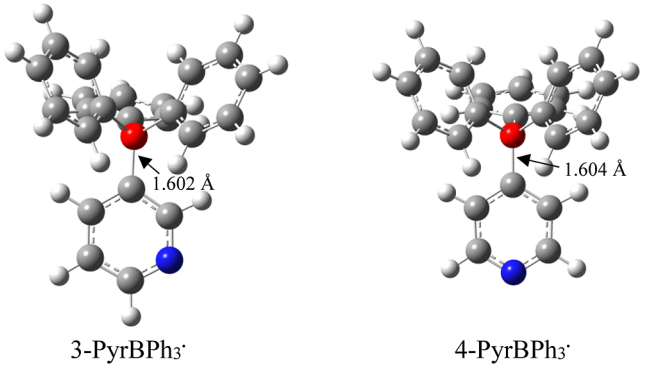

Figure 3. M06-2X/aug-*cc*-pVTZ optimized structures of 3-Pyr$BPh_3^\bullet$ and 4-Pyr$BPh_3^\bullet$ where bond lengths are given in Å.

instead it contracts from 1.643 (3-PyrBPh_3^-) and 1.639 Å (4-PyrBPh_3^-) to 1.602 (3-Pyr$BPh_3^\bullet$) and 1.604 (4-Pyr$BPh_3^\bullet$) Å; subsequent computations on radicals with the phenyl ring substituents included lead to similar results (Figures S2). This suggests that cleavage of BAr_3 versus BF_3 from the anions is energetically similar, whereas for the neutral species the former process takes more energy than the latter one. In accord with this conclusion, the 0 K CCSD(T)/maug-*cc*-pVTZ dissociation enthalpies are 75.2 and 74.4 kcal mol^{-1} for 3-PyrBPh_3^-

https://doi.org/10.1021/acs.jpca.3c04479
J. Phys. Chem. A 2023, 127, 8828−8833

and 4-PyrBPh$_3^-$, and 12.2 and 10.8 kcal mol^{-1} for the corresponding radicals; interestingly, cleavage of phenyl radical from the two neutral structures (10.8 and 11.8 kcal mol^{-1}, respectively) is energetically similar despite the presence of a ∼ 0.5 Å longer C_{phenyl}–B bond.

M06-2X/aug-*cc*-pVTZ computed VDEs for anions **3**$^-$–**6**$^-$ span a 0.33 eV range from 4.51 eV (**5**$^-$) to 4.84 eV (**6**$^-$) (Table 1). These calculated values are in excellent accord with the observed results [i.e., 4.77 (calc) vs 4.65 (expt) eV (**3**$^-$), 4.76 (calc) vs 4.66 (expt) eV (**4**$^-$), 4.51 (calc) vs 4.50 (expt) eV (**5**$^-$), and 4.84 (calc) vs 4.90 (expt) eV (**6**$^-$)]. They also reveal that 4-PyrB(4-MeOC$_6$H$_4$)$_3^-$ is the most electron rich anion (i.e., the one with the lowest VDE), two methoxy groups at the 3,5-positions of the benzene ring are electron withdrawing, and all four pyridyltriarylborate anions are ∼1.0 eV easier to oxidize than 3- and 4-pyridyltrifluoroborate. Their ADEs [4.06 (**3**$^-$), 4.10 (**4**$^-$), 3.91 (**5**$^-$), and 4.52 (**6**$^-$) eV] are ∼0.5 eV smaller than the VDEs which is consistent with large geometry changes upon photodetachment and our assigned ADEs of ≤4.1 (**3**$^-$), ≤4.2 (**4**$^-$), ≤4.1 (**5**$^-$), and ≤4.3 (**6**$^-$) eV.

The VDEs of **1**$^-$–**6**$^-$ provide an indication of their valence electron density and may also reflect the nucleophilicity of these ions. Their experimental values were consequently compared to the rate constants for the S_N2 reactions of **1**–**4** and **6** with 1-iodooctane in dichloromethane; **5** is omitted because its rate constant was not reported.[32] A linear correlation is observed between the logarithm of the S_N2 rate constants and the VDEs (Figure 4) and a least-squares

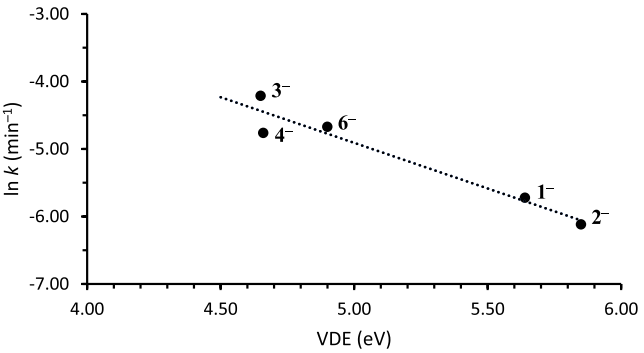

Figure 4. Plot of ln *k* for the reactions of the PPh_4^+ salts of **1**$^-$–**4**$^-$ and **6**$^-$ with 1-iodooctane vs the observed VDEs for the corresponding anions. The respective VDE (eV) and ln *k* (min^{-1})[32] values for each anion follow: 5.64 and −5.72 (**1**$^-$); 5.85 and −6.12 (**2**$^-$); 4.65 and −4.21 (**3**$^-$); 4.66 and −4.76 (**4**$^-$); and 4.90 and −4.67 (**6**$^-$).

analysis of the data affords ln *k* (min^{-1}) = −1.35 × VDE (eV) + 1.85, r^2 = 0.934. Similar plots of ln *k* vs the highest occupied molecular orbital (HOMO) and the highest-one occupied molecular orbital (HOMO-1) energies of the anions are also linear; ln *k* (min^{-1}) = 2.87 × HOMO (eV) + 7.85, r^2 = 0.910 and ln *k* (min^{-1}) = 2.78 × HOMO-1 (eV) + 7.68, r^2 = 0.931 (Figures S3 and S4).[46]

These results might be considered surprising since the reactivity of **1**–**6** are counterion-dependent and were determined in a nonpolar solvent,[32] whereas the VDEs were measured in the gas phase for the free anions in the absence of a solvent or counterion. This is not the first time, however, that gas phase measurements and computations on free anions have been found to correlate with the behavior of organic salts in nonpolar solvents.[6,32,47]

Spin densities for **1**•–**6**• were visualized (Figure S5) and correspond to σ (**1**• and **2**•) and π (**3**•–**6**•) radicals, with the unpaired electron primarily residing in the substituted phenyl rings in the latter species. This is similar to the HOMO and HOMO−1 of **1**$^-$–**6**$^-$, and it suggests that both cation–π and nitrogen lone-pair–cation interactions are important in the salts of these anions.

CONCLUSIONS

A series of 6 arylborate anions **1**$^-$–**6**$^-$ were examined by NIPES at 20 K and the VDEs for the aryltrifluoroborates [3-PyrBF$_3^-$ (5.64 eV) and 4-PyrBF$_3^-$ (5.85 eV)] are ∼1.0 eV higher than the 3-PyrB(4-*t*-BuC$_6$H$_4$)$_3^-$ and 4-PyrBAr$_3^-$ [Ar = 4-*t*-BuC$_6$H$_4$, 4-MeOC$_6$H$_4$, 3,5-(MeO)$_2$C$_6$H$_3$] derivatives, which span from 4.50–4.90 eV. This indicates that the pyridyltriarylborate anions are electron-rich relative to their BF_3 analogues which is in accord with the greater reactivity of their tetraphenylphosphonium ion salts, and a linear correlation between the measured VDEs and ln *k* for their S_N2 reaction with 1-iodooctane in CH_2Cl_2.

Computations reproduce the experimental VDEs and provide structures for both borate anions and their corresponding neutral structures. The resulting spin densities of the radicals and HOMO and HOMO-1 of **1**$^-$–**6**$^-$ reveal that photodetachment of an electron from the nitrogen lone pair or the π system of an aryl group takes place. This suggests that these are the locations where a cation interacts with these anions and provides a basis for modifying the latter structures to weaken the attractive interactions between the oppositely charged species.

ASSOCIATED CONTENT

Data Availability Statement

The data underlying this study are available in the published article and its Supporting Information.

Supporting Information

The Supporting Information is available free of charge at https://pubs.acs.org/doi/10.1021/acs.jpca.3c04479.

Computed and experimental VDEs and ADEs; fragmentation energies of **1**$^-$–**6**$^-$ and their corresponding radicals; illustrated structures of 3-PyrBPh$_3^-$, 4-PyrBPh$_3^-$, **3**$^-$–**6**$^-$, and their corresponding radicals; plots of ln *k* versus HOMO and HOMO-1 energies; illustrated spin densities of **1**•–**6**•; *xyz* coordinates; and energies for all of the calculated structures (PDF)

AUTHOR INFORMATION

Corresponding Authors

Xue-Bin Wang – *Physical Sciences Division, Pacific Northwest National Laboratory, Richland, Washington 99352, United States;* orcid.org/0000-0001-8326-1780; Email: xuebin.wang@pnnl.gov

Steven R. Kass – *Department of Chemistry, University of Minnesota, Minneapolis, Minnesota 55455, United States;* orcid.org/0000-0001-7007-9322; Email: kass@umn.edu

Authors

Stephen H. Dempsey – *Department of Chemistry, University of Minnesota, Minneapolis, Minnesota 55455, United States*

Wenjin Cao – *Physical Sciences Division, Pacific Northwest National Laboratory, Richland, Washington 99352, United States;* orcid.org/0000-0002-2852-4047

https://doi.org/10.1021/acs.jpca.3c04479
J. Phys. Chem. A 2023, 127, 8828–8833

Complete contact information is available at:
https://pubs.acs.org/10.1021/acs.jpca.3c04479

Notes

The authors declare no competing financial interest.

■ ACKNOWLEDGMENTS

Generous support from the National Science Foundation (CHE-1955186), the donors of the American Chemical Society Petroleum Research Fund (ACS PRF 65096-ND4), and the Minnesota Supercomputing Institute for Advanced Computational Research are gratefully acknowledged. The photoelectron spectra work was supported by U.S. Department of Energy (DOE), Office of Science, Office of Basic Energy Sciences, Division of Chemical Science, Geosciences, and Biosciences, Condensed Phase and Interfacial Molecular Science program, FWP 16248.

■ REFERENCES

(1) Shaik, S.; Danovich, D.; Joy, J.; Wang, Z.; Stuyver, T. Electric-Field Mediated Chemistry: Uncovering and Exploiting the Potential of (Oriented) Electric Fields to Exert Chemical Catalysis and Reaction Control. *J. Am. Chem. Soc.* **2020**, *142*, 12551−12562.
(2) Ciampi, S.; Darwish, N.; Aitken, H. M.; Díez-Pérez, I.; Coote, M. L. Harnessing Electrostatic Catalysis in Single Molecule, Electrochemical and Chemical Systems: A Rapidly Growing Experimental Tool Box. *Chem. Soc. Rev.* **2018**, *47*, 5146−5164.
(3) Shaik, S.; Ramanan, R.; Danovich, D.; Mandal, D. Structure and Reactivity/Selectivity Control by Oriented-External Electric Fields. *Chem. Soc. Rev.* **2018**, *47*, 5125−5145.
(4) Stuyver, T.; Danovich, D.; Joy, J.; Shaik, S. External Electric Field Effects on Chemical Structure and Reactivity. *Wiley Interdiscip. Rev.: Comput. Mol. Sci.* **2020**, *10* (1−22), No. e1438.
(5) Mondal, T.; Shaik, S.; Kenttämaa, H.; Stuyver, T. Modulating the Radical Reactivity of Phenyl Radicals with the Help of Distonic Charges: It is All About Electrostatic Catalysis. *Chem. Sci.* **2021**, *12*, 4800−4809.
(6) Samet, M.; Buhle, J.; Zhou, Y.; Kass, S. R. Charge-Enhanced Acidity and Catalyst Activation. *J. Am. Chem. Soc.* **2015**, *137*, 4678−4680.
(7) Fan, Y.; Kass, S. R. Electrostatically Enhanced Thioureas. *Org. Lett.* **2016**, *18*, 188−191.
(8) Ma, J.; Kass, S. R. Electrostatically Enhanced Phosphoric Acids: A Tool in Brønsted Acid Catalysis. *Org. Lett.* **2016**, *18*, 5812−5815.
(9) Fan, Y.; Kass, S. R. Enantioselective Friedel-Crafts Alkylation between Nitroalkenes and Indoles Catalyzed by Charge Activated Thiourea Organocatalysts. *J. Org. Chem.* **2017**, *82*, 13288−13296.
(10) Ma, J.; Kass, S. R. Asymmetric Arylation of 2,2,2-Trifluoroacetophenones Catalyzed by Chiral Electrostatically-Enhanced Phosphoric Acids. *Org. Lett.* **2018**, *20*, 2689−2692.
(11) Fan, Y.; Tiffner, M.; Schörgenhumer, J.; Robiette, R.; Waser, M.; Kass, S. R. Synthesis of Cyclic Organic Carbonates Using Atmospheric Pressure CO_2 and Charge-Containing Thiourea Catalysts. *J. Org. Chem.* **2018**, *83*, 9991−10000.
(12) Fan, Y.; Payne, C.; Kass, S. R. Quantification of Catalytic Activity for Electrostatically Enhanced Thioureas via Reaction Kinetics and UV−vis Spectroscopic Measurement. *J. Org. Chem.* **2018**, *83*, 10855−10863.
(13) Ma, J.; Kass, S. R. Electrostatically Enhanced Phosphoric Acids and Their Applications in Asymmetric Friedel-Crafts Alkylations. *J. Org. Chem.* **2019**, *84*, 11125−11134.
(14) Riegel, G. F.; Kass, S. R. N-Vinyl and N-Aryl Hydroxypyridinium Ions: Charge-Activated Catalysts with Electron Withdrawing Groups. *J. Org. Chem.* **2020**, *85*, 6017−6026.
(15) Payne, C.; Kass, S. R. Structural Considerations for Charge-Enhanced Brønsted Acid Catalysts. *J. Phys. Org. Chem.* **2020**, *33* (1−16), No. e4069.
(16) Riegel, G. F.; Payne, C.; Kass, S. R. Effects of Brønsted Acid Co-Catalysts on the Activities and Selectivities of Charge-Enhanced Thiourea Organocatalysts in Friedel-Crafts and Oxa-Pictet-Spengler Reactions. *J. Phys. Org. Chem.* **2022**, *35* (1−12), No. e4321.
(17) Riegel, G. F.; Takashige, K.; Lovstedt, A.; Kass, S. R. Charge-Activated TADDOLs: Recyclable Organocatalysts for Asymmetric (Hetero-)Diels-Alder Reactions. *J. Phys. Org. Chem.* **2022**, *35* (1−13), No. e4355.
(18) Blechschmidt, D. R.; Lovstedt, A.; Kass, S. R. Metallocenium Lewis Acid Catalysts for Use in Friedel-Crafts Alkylation and Diels-Alder Reactions. *Organometallics* **2022**, *41*, 2648−2655.
(19) Smajlagic, I.; White, B.; Azeez, O.; Pilkington, M.; Dudding, T. Organocatalysis Linked to Charge-Enhanced Acidity with Super-electrophilic Traits. *ACS Catal.* **2022**, *12*, 1128−1138.
(20) Smajlagic, I.; Guest, M.; Durán, R.; Herrera, B.; Dudding, T. Mechanistic Insight toward Understanding the Role of Charge in Thiourea Organocatalysis. *J. Org. Chem.* **2020**, *85*, 585−593.
(21) Chen, L.; Xiao, B.-X.; Du, W.; Chen, Y.-C. Quaternary Phosphonium Salts as Active Brønsted Acid Catalysts for Friedel−Crafts Reactions. *Org. Lett.* **2019**, *21*, 5733−5736.
(22) Anzabi, M. Y.; Yazdani, H.; Bazgir, A. Electrostatically Enhanced Sulfuric Acid: A Strong Brønsted Acidic Catalyst for Multi-Component Reactions. *Catal. Lett.* **2019**, *149*, 1934−1940.
(23) Rostami, A.; Mahmoodabadi, M.; Hossein Ebrahimi, A.; Khosravi, H.; Al-Harrasi, A. An Electrostatically Enhanced Phenol as a Simple and Efficient Bifunctional Organocatalyst for Carbon Dioxide Fixation. *ChemSusChem* **2018**, *11*, 4262−4268.
(24) Steglich, W.; Höfle, G. *N*, *N*-Dimethyl-4-Pyridinamine, a Very Effective Acylation Catalyst. *Angew. Chem., Int. Ed.* **1969**, *8*, 981.
(25) Höfle, G.; Steglich, W.; Vorbrüggen, H. 4-Dialkylaminopyridines as Highly Active Acylation Catalysts. [New Synthetic Method (25)]. *Angew. Chem., Int. Ed.* **1978**, *17*, 569−583.
(26) Heinrich, M. R.; Klisa, H. S.; Mayr, H.; Steglich, W.; Zipse, H. Enhancing the Catalytic Activity of 4-(Dialkylamino)Pyridines by Conformational Fixation. *Angew. Chem., Int. Ed.* **2003**, *42*, 4826−4828.
(27) Palomo, C.; Oiarbide, M.; Lopez, R. Asymmetric Organocatalysis by Chiral Bronsted Bases: Implications and Applications. *Chem. Soc. Rev.* **2009**, *38*, 632−653.
(28) Fu, X.; Tan, C.-H. Mechanistic Considerations of Guanidine-Catalyzed Reactions. *Chem. Commun.* **2011**, *47*, 8210−8222.
(29) Roughley, S. D.; Jordan, A. M. The Medicinal Chemist's Toolbox: An Analysis of Reactions Used in the Pursuit of Drug Candidates. *J. Med. Chem.* **2011**, *54*, 3451−3479.
(30) Soderberg, T. "Organic Chemistry with a Biological Emphasis", 2019, LibreTexts Chemistry, https://digitalcommons.morris.umn.edu/chem_facpubs/1/(9/6/23) and https://digitalcommons.morris.umn.edu/chem_facpubs/2/(acessed date 9-6-23).
(31) Boddu, S. K.; Ur Rehman, N.; Mohanta, T. K.; Majhi, A.; Avula, S. K.; Al-Harrasi, A. A Review on DBU-Mediated Organic Transformations. *Green Chem. Lett. Rev.* **2022**, *15*, 765−795.
(32) Dempsey, S. H.; Lovstedt, A.; Kass, S. R. Electrostatically Enhanced 3- and 4-Pyridyl Borate Salt Nucleophiles and Bases. *J. Org. Chem.* **2023**, *88*, 10525−10538.
(33) The reactivity ratio is concentration-dependent and the given ratio was obtained using 50 mM 1-butanol, 100 mM 4-methylisocyanate, and 10 mM of **3** as the catalyst. For further details, see ref 32.
(34) Yuan, Q.; Cao, W.; Wang, X.-B. Cryogenic and Temperature-Dependent Photoelectron Spectroscopy of Metal Complexes. *Int. Rev. Phys. Chem.* **2020**, *39*, 83−108.
(35) Hanstorp, D.; Gustafsson, M. Determination of the Electron Affinity of Iodine. *J. Phys. B: At., Mol. Opt. Phys.* **1992**, *25*, 1773−1783.
(36) Wang, X.-B.; Wang, Y.-L.; Yang, J.; Xing, X.-P.; Li, J.; Wang, L.-S. Evidence of Significant Covalent Bonding in $Au(CN)_2^-$. *J. Am. Chem. Soc.* **2009**, *131*, 16368−16370.
(37) Zhao, Y.; Truhlar, D. G. How Well Can New-Generation Density Functionals Describe the Energetics of Bond-Dissociation

Reactions Producing Radicals? *J. Phys. Chem. A* **2008**, *112*, 1095−1099.
(38) Zhao, Y.; Truhlar, D. G. The M06 Suite of Density Functionals for Main Group Thermochemistry, Thermochemical Kinetics, Noncovalent Interactions, Excited States, and Transition Elements: Two New Functionals and Systematic Testing of Four M06-Class Functionals and 12 Other Functionals. *Theor. Chem. Acc.* **2008**, *120*, 215−241.
(39) Zhao, Y.; Truhlar, D. G. Density Functionals with Broad Applicability in Chemistry. *Acc. Chem. Res.* **2008**, *41*, 157−167.
(40) Dunning, T. H., Jr. Gaussian Basis Sets for Use in Correlated Molecular Calculations. I. The Atoms Boron Through Neon and Hydrogen. *J. Chem. Phys.* **1989**, *90*, 1007−1023.
(41) Papajak, E.; Truhlar, D. G. Efficient Diffuse Basis Sets for Density Functional Theory. *J. Chem. Theory Comput.* **2010**, *6*, 597−601.
(42) Purvis, G. D.; Bartlett, R. J. A Full Coupled-Cluster Singles and Doubles Model: The Inclusion of Disconnected Triples. *J. Chem. Phys.* **1982**, *76*, 1910−1918.
(43) Watts, J. D.; Bartlett, R. J. The Coupled-Cluster Single, Double, and Triple Excitation Model for Open-Shell Single Reference Functions. *J. Chem. Phys.* **1990**, *93*, 6104−6105.
(44) Frisch, M. J.; Trucks, G. W.; Schlegel, H. B.; Scuseria, G. E.; Robb, M. A.; Cheeseman, J. R.; Scalmani, G.; Barone, V.; Petersson, G. A.; Nakatsuji, H.; Li, X.; Caricato, M.; Marenich, A. V.; Bloino, J.; Janesko, B. G.; Gomperts, R.; Mennucci, B.; Hratchian, H. P.; Ortiz, J. V.; Izmaylov, A. F.; Sonnenberg, J. L.; Williams-Young, D.; Ding, F.; Lipparini, F.; Egidi, F.; Goings, J.; Peng, B.; Petrone, A.; Henderson, T.; Ranasinghe, D.; Zakrzewski, V. G.; Gao, J.; Rega, N.; Zheng, G.; Liang, W.; Hada, M.; Ehara, M.; Toyota, K.; Fukuda, R.; Hasegawa, J.; Ishida, M.; Nakajima, T.; Honda, Y.; Kitao, O.; Nakai, H.; Vreven, T.; Throssell, K.; Montgomery, J. A., Jr.; Peralta, J. E.; Ogliaro, F.; Bearpark, M. J.; Heyd, J. J.; Brothers, E. N.; Kudin, K. N.; Staroverov, V. N.; Keith, T. A.; Kobayashi, R.; Normand, J.; Raghavachari, K.; Rendell, A. P.; Burant, J. C.; Iyengar, S. S.; Tomasi, J.; Cossi, M.; Millam, J. M.; Klene, M.; Adamo, C.; Cammi, R.; Ochterski, J. W.; Martin, R. L.; Morokuma, K.; Farkas, O.; Foresman, J. B.; Fox, D. J. *Gaussian 16*; Gaussian, Inc.: Wallingford, CT, 2016.
(45) Dennington, R.; Keith, T.; Millam, J. *GaussView*. Version 6; Semichem Inc.: Shawnee Mission, KS, 2016.
(46) It is interesting to note that a similar linear correlation is observed between the experimental VDE and the computed HOMO [i.e., VDE (eV) = −1.77 × HOMO (eV) − 2.81, r^2 = 0.917], and an even better one is obtained with the HOMO - 1 [i.e., VDE (eV) = −1.90 × HOMO − 1 (eV) − 3.57, r^2 = 0.977].
(47) Dempsey, S. H.; Kass, S. R. Liberating the Anion: Evaluating Weakly Coordinating Cations. *J. Org. Chem.* **2022**, *87*, 15466−15482.

https://doi.org/10.1021/acs.jpca.3c04479
J. Phys. Chem. A 2023, 127, 8828−8833